



# Kinetic Driver of Antibacterial Drugs against *Plasmodium falciparum* and Implications for Clinical Dosing

Emily Caton,<sup>a\*</sup> Elizabeth Nenortas,<sup>a</sup> Rahul P. Bakshi,<sup>a,b</sup> Theresa A. Shapiro<sup>a,b</sup>

<sup>a</sup>Division of Clinical Pharmacology, Departments of Medicine and of Pharmacology and Molecular Sciences, The Johns Hopkins University School of Medicine, Baltimore, Maryland, USA

<sup>b</sup>The Johns Hopkins Malaria Research Institute, The Johns Hopkins University Bloomberg School of Public Health, Baltimore, Maryland, USA

**ABSTRACT** Antibacterial drugs are an important component of malaria therapy. We studied the interactions of clindamycin, tetracycline, chloramphenicol, and ciprofloxacin against *Plasmodium falciparum* under static and dynamic conditions. In microtiter plate assays (static conditions), and as expected, parasites displayed the delayed death response characteristic for apicoplast-targeting drugs. However, rescue by isopentenyl pyrophosphate was variable, ranging from 2,700-fold for clindamycin to just 1.7-fold for ciprofloxacin, suggesting that ciprofloxacin has targets other than the apicoplast. We also examined the pharmacokinetic-pharmacodynamic relationships of these antibacterials in an *in vitro* glass hollow-fiber system that exposes parasites to dynamically changing drug concentrations. The same total dose and area under the concentration-time curve (AUC) of the drug was deployed either as a single short-lived high peak (bolus) or as a constant low concentration (infusion). All four antibacterials were unambiguously time-driven against malaria parasites: infusions had twice the efficacy of bolus regimens, for the same AUC. The time-dependent efficacy of ciprofloxacin against malaria is in contrast to its concentration-driven action against bacteria. *In silico* simulations of clinical dosing regimens and resulting pharmacokinetics revealed that current regimens do not maximize time above the MICs of these drugs. Our findings suggest that simple and rational changes to dosing may improve the efficacy of antibacterials against falciparum malaria.

**KEYWORDS** *Plasmodium falciparum*, malaria, pharmacokinetics, pharmacodynamics, PK/PD, clindamycin, tetracycline, doxycycline, chloramphenicol, ciprofloxacin, chemotherapy

Despite considerable recent success in global control efforts, *Plasmodium falciparum* malaria remains a major public health problem. Billions of people are at risk of infection, approximately 200 million are infected annually, and almost half a million die, most of them young children (1). The parasite has become resistant to many antimalarials, limiting their use for treatment in large parts of Africa and Asia. Artemisinins form the last line of defense; however, the recent emergence of the *PfKelch13* mutant parasites with delayed response threatens this entire drug class (2). The need to discover new drugs and improve the efficacy of existing agents is pressing.

The antimalarial activity of antibacterials was recognized early, with first reports in the mid-1930s for prontosil and sulfonamides (3, 4), followed in the late 1940s by chloramphenicol (CHL) and tetracyclines (5). Long regarded as clinically irrelevant because of their slow action and the availability of superior chloroquine, the utility of antibacterials was reevaluated upon the emergence and rapid worldwide spread of chloroquine resistance (6–8). Reflecting the current inadequacy of antimalarial therapy, antibacterial drugs, including clindamycin (CLI) and the tetracyclines, are now important components of the antimalarial armamentarium that are commonly used as

**Citation** Caton E, Nenortas E, Bakshi RP, Shapiro TA. 2019. Kinetic driver of antibacterial drugs against *Plasmodium falciparum* and implications for clinical dosing. *Antimicrob Agents Chemother* 63:e00416-19. <https://doi.org/10.1128/AAC.00416-19>.

**Copyright** © 2019 American Society for Microbiology. All Rights Reserved.

Address correspondence to Theresa A. Shapiro, [tshapiro@jhmi.edu](mailto:tshapiro@jhmi.edu).

\* Present address: Emily Caton, Zeteo Tech, Inc., Sykesville, Maryland, USA.

**Received** 25 February 2019

**Returned for modification** 24 April 2019

**Accepted** 7 August 2019

**Accepted manuscript posted online** 26 August 2019

**Published** 22 October 2019

**TABLE 1** Pharmacokinetics of antibacterials

Drug	Antibacterial target	PK driver vs bacteria (11, 53)	Plasma $t_{1/2}$ (h) (21)
Clindamycin	70S ribosome, 50S subunit	Time	3
Tetracycline	70S ribosome, 30S subunit	Time	6–11
Chloramphenicol	70S ribosome, 50S subunit	Time	3
Ciprofloxacin	DNA gyrase, topoisomerase IV	Concn	4

monotherapy for prophylaxis or in combinations for the treatment of established infection (9).

Against bacteria the efficacy of antibacterials is driven, in a class-wide manner (Table 1), by either concentration or time of exposure (10–14). The same total dose and drug exposure (area under the concentration-time curve [AUC]) can be deployed via dosing regimens that emphasize either concentration or time of exposure (Fig. 1A). The pharmacodynamic (PD) efficacy of a given regimen depends on whether concentration or time of exposure is the governing pharmacokinetic (PK) parameter, a relationship clearly recognized and enunciated early in the antibiotic era (15, 16). Clinical dosing of antibacterials is accordingly based on kinetic driver: short-lived penicillins (which are time dependent) are dosed continuously, whereas equally short-lived but concentration-dependent aminoglycosides are dosed just once daily. Although perhaps counterintuitive, repeated dosing of aminoglycosides to obtain more sustained plasma levels results in reduced, not improved, efficacy, as well as severe toxicities (17, 18). The kinetic driver of a drug's efficacy must be determined empirically and is unrelated to "static" versus "cidal" activity, reversible versus irreversible inhibition, targeted pathway, or chemical structure. Time-kill curves, which variably capture any post-anti-infective response, may not faithfully reflect kinetic governance (10). The kinetic driver of antibacterial action is, however, the same across a therapeutic class of agents (e.g., all aminoglycosides are concentration-driven), and we recently demonstrated this to be so for antitrypanosomals (19).

Using a novel apparatus that can deploy, *in vitro*, dynamically changing drug concentrations against *P. falciparum*, we demonstrated that the concept of efficacy-governing PK driver (either concentration or time) is also applicable to antimalarial drugs (19, 20). The remarkable activity of short-lived artemisinins (with plasma half-lives

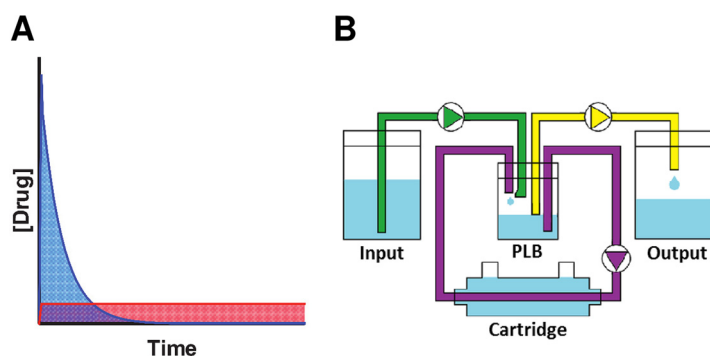


**FIG 1** Dynamic pharmacokinetics as seen *in vivo* can be obtained *in vitro*. (A) After a single dose of drug at  $t_0$ , the concentration in blood (blue) rises to a maximum and then falls at a characteristic rate ( $t_{1/2}$ ). The AUC (blue shaded), an index of drug exposure, is proportional to the dose. The same total dose and AUC can be deployed by two extreme pharmacokinetic regimens that emphasize either concentration or time. A single bolus (blue) achieves high concentration over a short time, whereas a constant infusion (red) provides low concentration for prolonged time. Difference in the outcome of the same AUC by these distinctive regimens reveals the pharmacokinetic driver of efficacy: either concentration or time of exposure. (B) Schematic of the dynamic *in vitro* PK/PD system. A cylindrical glass cartridge, traversed by semipermeable dialysis tubing, houses parasitized erythrocytes (PD compartment). Medium flows continuously in the closed primary loop circuit (purple) and equilibrates with that in the PD compartment. Dynamic drug concentrations are created by fluids that are pumped (arrowheads) into and out of (green and yellow tubing, respectively) the primary loop bottle (PLB).

$[t_{1/2}]$  in humans of just 1 to 2 h) is made possible by their concentration-driven efficacy (20, 21). The dosing strategy of antibacterials against *P. falciparum*, rooted in drivers and regimens against bacteria, raises the possibility that mediocre antimalarial activity may be due in part to differences in PK drivers between bacteria and parasites. Indeed, previous clinical trials of doxycycline have acknowledged a need to understand the pharmacokinetic variable most strongly associated with antimalarial activity in order to dose this drug optimally (22).

Among the many unusual features of malaria parasites is the fact that these eukaryotic cells contain two endosymbiotic organelles: the mitochondrion and the apicoplast, a relict nonphotosynthetic plastid (23, 24). Each cell thus has three genomes, three sets of tRNAs, three sets of rRNAs, and three complements of enzymatic machinery for replicating DNA and transforming its genetic code into proteins. For the mitochondrion and apicoplast, the genes for many of these components have been transferred to the nucleus, but key elements remain encoded by the prokaryote-like organelle genomes, and the imported proteins retain their prokaryote character. The 35-kb circular apicoplast genome has 50 to 60 genes encoding rRNA, tRNA, RNA polymerase subunits, essential ribosomal proteins, and transcription/translation factors (24, 25). In addition, the apicoplast houses prokaryote-like metabolic pathways, including one for isoprenoid biosynthesis that is essential for *falciparum* survival (26, 27). Efficacy of antibacterials against *P. falciparum* is believed to be largely due to the susceptibility of prokaryote-like apicoplast components and processes to these drugs (28).

In erythrocytic malaria parasites, a notable consequence of targeting metabolic machinery in the apicoplast is the phenomenon of “delayed death” (28–30). Parasites with compromised apicoplasts can complete the ongoing 48-h replication cycle; however, absence of the organelle and/or its products blocks growth in the subsequent cycle, leading to a delayed impact on parasite number (28). *In vitro*, this manifests as significantly better efficacy when drug exposure in the assay is extended over multiple 48-h life cycles. Delayed death is a hallmark of compounds targeting the apicoplast and in turn is used as indicative of the mode of action of compounds with unknown mechanisms (31). Importantly, apicoplast depletion in erythrocytic parasites can, for some time, be compensated for by supplying exogenous isopentenyl pyrophosphate (IPP), a product of apicoplast metabolism and the precursor for all isoprenoid biosynthesis in the parasite (26, 27). IPP rescue is considered a confirmation of apicoplast targeting by a test compound.

We utilized our glass hollow-fiber *in vitro* PK/PD system (Fig. 1B) to determine the PK driver that governs the antimalarial activity of clindamycin (CLI), tetracycline (TET), chloramphenicol (CHL), and ciprofloxacin (CIP). We examined whether the kinetic governance of these drugs is different in malaria versus bacteria, and we simulated current dosing regimens *in silico* to explore the implications of the PK driver for the clinical use of antibacterials in malaria.

## RESULTS

**Delayed death and IPP rescue.** All antibacterials tested were active against parasites in standard 72-h microtiter plate assays, with mean 50% effective concentrations ( $EC_{50}$ s) of 0.025 to 16  $\mu$ M (Table 2). Lengthening the exposure time to 96 h consistently increased the efficacy 1.5- to 2.3-fold, in keeping with an apicoplast-mediated effect and delayed-death phenotype. This phenomenon is not seen for the artemisinins, antimalarials that do not target the apicoplast (Table 2). As expected from previous reports (26, 31), supplemental IPP reduced the potency of several antibacterials against *P. falciparum* (Fig. 2). The 72-h activity of CLI fell 2,700-fold with IPP (0.031 to 85  $\mu$ M), and the  $EC_{50}$ s of TET and CHL were changed 9-fold (1.4 to 13  $\mu$ M) and 6-fold (25 to 144  $\mu$ M), respectively. However, although statistically significant, the IPP rescue of CIP was marginal (3.6 to 6.1  $\mu$ M). There are several interesting features of these findings. First, the reversal by 200  $\mu$ M IPP is only partial: all four drugs retain antimalarial activity despite IPP. This suggests additional, nonapicoplast drug toxicities and/or insufficient

**TABLE 2** *In vitro* activities against *P. falciparum*

Drug	EC <sub>50</sub> (μM) <sup>a</sup>		Ratio
	72 h	96 h	
Clindamycin	0.025	0.012	2.1
Tetracycline	1.4	0.78	1.8
Doxycycline	2.1	0.90	2.3
Chloramphenicol	16.0	11.0	1.5
Ciprofloxacin	4.4	2.8	1.6
Artesunate	0.0031	0.0036	0.9
Artemisinin	0.0091	0.0082	1.1

<sup>a</sup>Each EC<sub>50</sub> value was obtained from ≥3 independent experiments (45 total experiments). All %CV values were ≤19. In 45 experiments, the R<sup>2</sup> values in unweighted analyses were ≥0.9719 (mean, 0.9893).

replenishment of charged isopentenyl pyrophosphate at its sites of need. The second is a variance in the degree of reversal, which was profound for CLI but substantially less marked for TET and CHL. This is also consistent with additional nonapicoplast toxicities (which may vary from drug to drug), especially for TET and CHL (32–34). Finally, despite having a classic delayed death effect on malaria parasites, the activity of DNA gyrase poison CIP was relatively unaffected by IPP supplementation, which changed the EC<sub>50</sub> value by <2-fold (Fig. 2D). This fluoroquinolone in particular is known to have non-apicoplast targets in malaria parasites (35).

#### Dynamic *in vitro* pharmacokinetics/pharmacodynamics: system performance.

Standardized artificial kinetics were deployed in our *in vitro* apparatus to identify the governing PK driver of antimalarial activity. Initial experiments with cognate radiolabeled drug tracers indicated that for all four antibacterials, nonspecific drug binding to the system was <10% and that programmed kinetics were indeed achieved. All obtained half-lives were within 10% of desired (Fig. 3, top panels). In a total of 24 PK/PD experiments comprising 73 cartridges, three experiments were discarded because of system hardware problems or contamination. In 21 successful studies, the final percent parasitemias in untreated control cartridges were 4.8 ± 0.41 (72 h) and 5.1 ± 1.7 (96 h).

**Identification of the kinetic driver.** For a given drug, the same total dose and AUC were deployed against parasites either as a constant infusion or as a bolus with a  $t_{1/2}$  of 4 h and a C<sub>max</sub> of 12.5× (72-h experiment) or 16.6× (96-h experiment) the infusion concentration. The experimental  $t_{1/2}$  of 4 h is comparable to half-lives obtained in humans for these antibacterials: CLI, 3 to 5 h; TET, 6 to 11 h; CHL, 2 to 4 h; and CIP, 4 to 6 h (Table 1). Assessing antibacterials by these means, with the conventional 72-h assay period (AUC<sub>0–72</sub>), showed no meaningful outcome difference between the regimens. The percent efficacies for bolus versus infusion were 25 versus 32, 37 versus 35, and 44 versus 38, for CLI, TET, and CIP, respectively. However, extending the

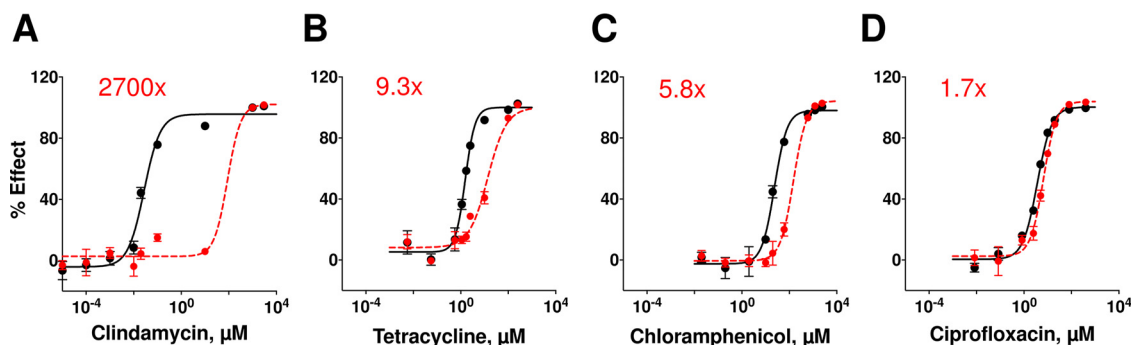


**FIG 2** The extent of rescue by IPP is variable. The simultaneous addition of 200 μM IPP with the test drug (dashed red curves) decreased the antimalarial efficacy of clindamycin (0.031 to 85 μM) (A), tetracycline (1.4 to 13 μM) (B), and chloramphenicol (25 to 144 μM) (C), evident as a rightward shift in the EC<sub>50</sub> in a 72-h cytotoxicity assay. (D) IPP had minimal effect on CIP activity (3.6 to 6.1 μM). Red text, fold change in EC<sub>50</sub> with IPP. The data are means ± standard deviations (some error bars are too small to extend outside their symbols; n = 4). All R<sup>2</sup> values were ≥0.97. The P values for cognate EC<sub>50</sub>s were all <0.02.

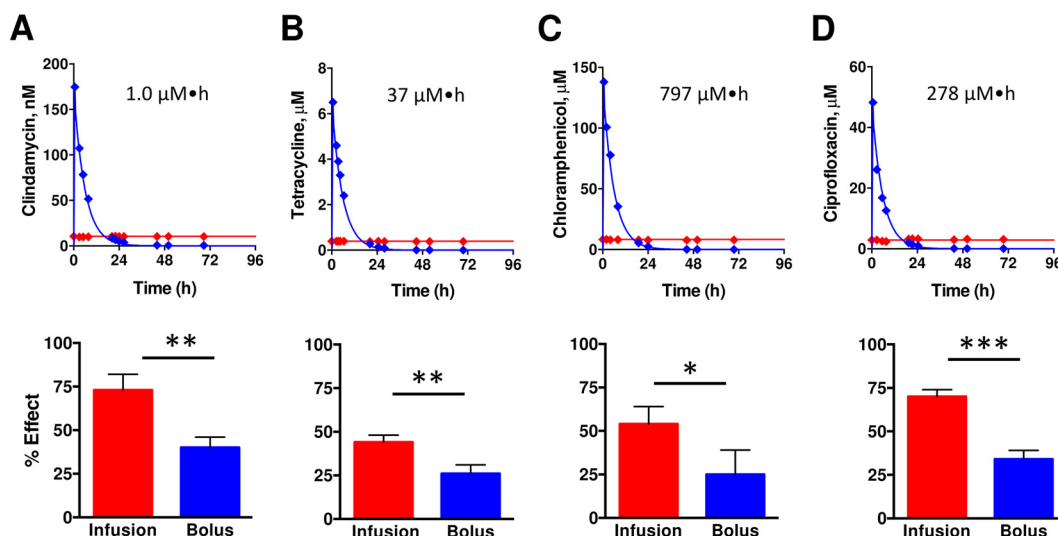


**FIG 3** Ninety-six-hour dynamic *in vitro* PK/PD to determine kinetic drivers against *P. falciparum*. (A to D) For the indicated drugs, concentrations in the PD compartment of a cartridge (where cells reside; top panels) were programmed prospectively (lines) and confirmed by cognate radiolabeled tracer (diamonds). For the indicated  $AUC_{0-96}$ , drug was deployed as a constant infusion (red) or bolus (blue) with  $C_{max}$  of  $16.6\times$  the infusion concentration and a  $t_{1/2}$  of 4 h. Corresponding PD outcomes (bottom panels) reveal that exposure to a transient high bolus (blue) was less effective than the same total dose and AUC provided as a constant low infusion (red). Values are means  $\pm$  the SD for  $n \geq 3$  experiments. \*,  $P \leq 0.05$ ; \*\*,  $P < 0.01$ ; \*\*\*,  $P = 0.001$  (Student *t* test).

experiments to 96 h ( $AUC_{0-96}$ ) provided sufficient life cycle coverage to reveal the time-driven action of these agents. For CLI, the bolus was 40% effective, while the infusion was 73%. Similarly, bolus was less effective than infusion for TET (26% versus 44%), CHL (25% versus 54%), and CIP (34% versus 70%) (Fig. 3, bottom panels). In each case, the same total dose and  $AUC_{0-96}$  was  $\sim 2$ -fold more effective when deployed as a constant infusion (time-intensive regimen) rather than as a high, rapidly cleared bolus (concentration-intensive regimen).

***In silico* simulation of pharmacokinetics in humans.** Time-dependent efficacy is maximized when trough concentrations of free drug in plasma are maintained above some therapeutic threshold, conventionally the MIC (here calculated as  $5\times$  the protein binding-adjusted *in vitro*  $EC_{50}$ ). We simulated the first 96-h plasma PK profiles of antibacterials dosed for an antimalarial indication: CLI and TET as currently recommended by the Centers for Disease Control and Prevention (9) and CHL and CIP as reported in malaria patients (36, 37). CLI is given at 7 mg/kg TID (three times daily; conventionally dosed at 0900, 1400, and 2100 h, with interdose intervals of 5, 7, and 12 h overnight). This regimen yields free-drug trough concentrations in plasma that exceed the MIC after the first dose and transiently fall below the MIC at the end of every 12 h overnight dosing break (Fig. 4A). The same total dose given every 8 h eliminates the 12-h overnight gap and maintains plasma CLI troughs above the MIC for the entire period (Fig. 4B).

For TET, achieving efficacious concentrations with QID dosing (four times daily, at 0900, 1300, 1700 and 2100 h) depends on simulated half-life, which in humans reportedly varies between 6 and 11 h (21). (The basis for this range is not well understood; TET is less than 5% metabolized (38); similar inconsistency is seen with relatively hydrophilic doxycycline but not with lipophilic minocycline (39), suggesting that variable absorption and distribution may contribute to this phenomenon.) With an 11-h half-life, plasma troughs do not exceed the MIC until after dose 6, approximately 30 h after the start of treatment, and two of every four subsequent troughs fall below the MIC (Fig. 4C). With a 6-h half-life, the TET concentrations never reach the MIC (Fig. 4C, inset). Modifying the dosing regimen to q6h (every 6 h), and with an 11-h half-life, improves the kinetics: once past the first 30 h, the troughs consistently exceed the MIC

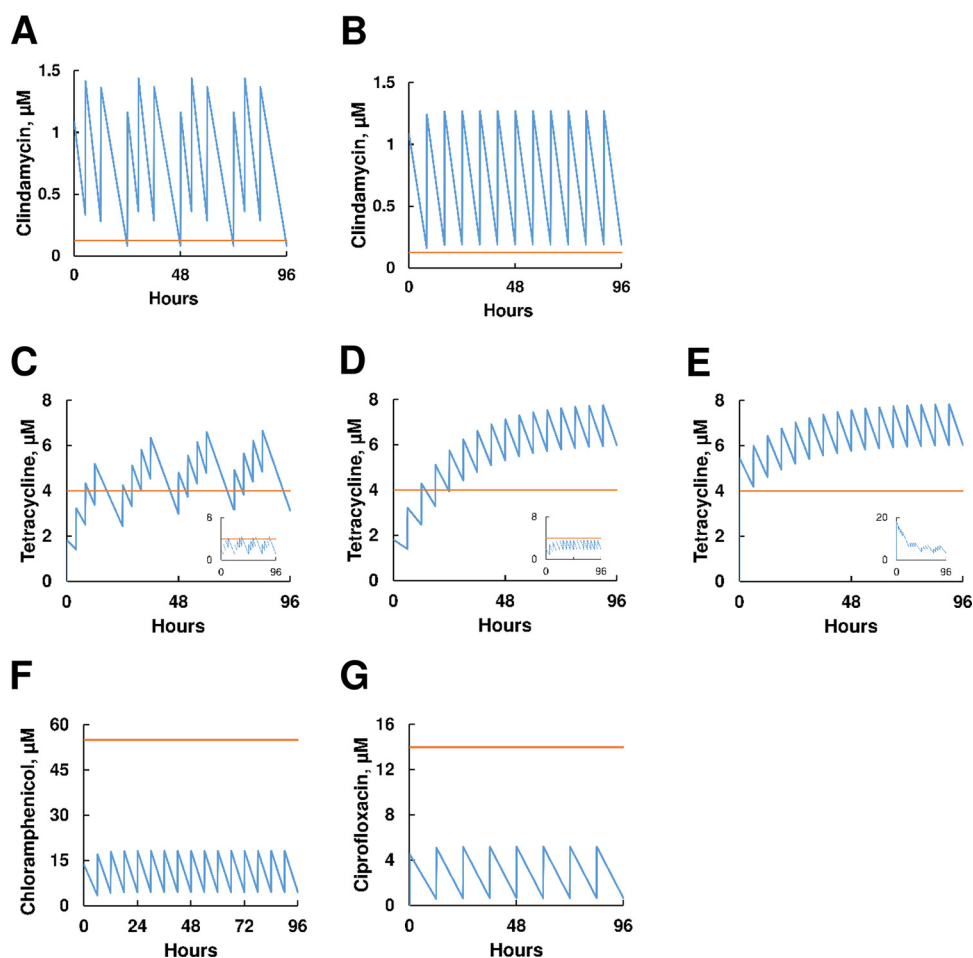


**FIG 4** Ninety-six-hour *in silico* PK simulation of antibacterials dosed for human malaria treatment. (A) CLI dosed at 7 mg/kg TID rapidly exceeds the MIC (0.125  $\mu\text{M}$ ) but transiently drops below it during 12-h overnight dosing breaks. (B) CLI dosed q8h maintains troughs above the MIC for the entire period. (C) TET dosed at 250 mg QID and with an 11-h half-life yields troughs that do not exceed the MIC (4  $\mu\text{M}$ ) until day 2 and that fall below the MIC after dosing breaks. TET with a 6-h half-life (inset) never exceeds the MIC. (D) TET dosed q6h and with an 11-h half-life yields troughs that exceed and remain above the MIC after 30 h. This regimen simulated with a 6-h half-life produces consistently subtherapeutic concentrations (inset). (E) After an initial 3 $\times$  loading dose of TET, followed by q6h dosing and an 11-h half-life, all troughs reliably exceed the MIC. Currently recommended QID TET dosing, even after (an unrealistic) 10 $\times$  loading dose and an 11-h half-life (inset), does not provide steady-state trough concentrations above the MIC. (F and G) CHL (25 mg/kg q6h, MIC = 55  $\mu\text{M}$ ) and CIP (750 mg q12h, MIC = 14  $\mu\text{M}$ ) plasma concentrations remain at a fraction of the MIC for the entire simulation period. Blue lines, simulated free drug concentration in plasma; red lines, MICs represented as 5 $\times$  protein binding-adjusted 96-h *in vitro* EC<sub>50</sub>.

(Fig. 4D). Again, if the half-life is only 6 h, efficacious plasma concentrations are not obtained (Fig. 4D, inset). The problem of subMIC concentrations during the first 30 h is solved by an initial loading dose three times the standard dose, which, in conjunction with q6h dosing (and an 11-h half-life) yields plasma concentrations that exceed the MIC after the first dose, and remain above it thereafter (Fig. 4E). Unfortunately, this strategy cannot salvage the conventional QID regimen, even with an 11-h half-life and 10-fold loading dose (Fig. 4E, inset).

Concentrations of CHL or CIP never reach the MIC (Fig. 4F and G) and toxicity issues preclude using doses large enough to remedy this problem (32, 34). Given the time dependence of antibacterials against *P. falciparum*, sustained concentrations above the MIC are of key importance. Though preliminary, these simulations provide a useful perspective on the therapeutic promise of these agents, at plasma concentrations expected from existing dosing regimens, and they suggest that simple dosing changes may boost antimalarial activity.

## DISCUSSION

These studies provide clear evidence that the antimalarial efficacy of the four studied antibacterials is time-driven *in vitro*: enhanced by constant presence above a therapeutic threshold. Though ostensibly logical that any antimalarial should continuously be kept above the MIC, time dependence of these agents is distinctly different from the concentration-driven artemisinins and experimental Hsp90 inhibitors, for which the same total dose and AUC are best deployed as a short-lived high concentration, despite many subsequent hours without meaningful drug levels, an *in vitro* finding confirmed in animals (19, 20). Interestingly, the time dependence of CIP efficacy against malaria parasites is unlike its concentration-driven action against bacteria (Table 1). Given the unpredictable and disconcertingly empirical nature of kinetic drivers of antiprotozoal activity (19, 40), perhaps the most important finding from these studies may stem from the seemingly trivial and self-evident fact that the common thread for antibacterials against malaria is that death is delayed, regardless of the more proximal molecular mechanisms of action (inhibition of protein synthesis or poisoning of DNA gyrase). Thus, the concentration or time dependence of a drug's action may be dictated by the eventual mechanism of death. Multiple death pathways have been described (e.g., necrosis or apoptosis) (41). They are downstream from the recognized molecular target, and they may involve multiple pathways that integrate at the level of an organelle. Although ciprofloxacin similarly poisons DNA topoisomerases in both bacteria and malaria parasites, the concentration-dependent action against bacteria, but time-dependent action against malaria, could be explained by differing death pathways that are triggered in these organisms.

Although their activity against the apicoplast is well characterized, several lines of evidence suggest that the antibacterials may have additional effects in malaria parasites. The highly variable and incomplete rescue by IPP (Fig. 2) could be explained by activities outside the apicoplast. Mitochondria seem a reasonable secondary target, given their prokaryotic origin, and the recognized mitochondrial toxicities of these drugs (32–34). Previous studies have documented retention of the *P. falciparum* mitochondrial genome in the face of doxycycline treatment (26, 31). This may be necessary but insufficient for proper mitochondrial function. Since critical metabolic machinery may be encoded in either the nucleus or the organelle and this distribution differs for apicoplast and mitochondrion (25, 42), the relative susceptibilities of these processes to antibacterial drugs are also likely to be disparate. More intriguing is the very limited rescue IPP provides against CIP toxicity, which suggests that DNA gyrase is required for the synthesis of some essential RNA that is not involved in the methylerythritol phosphate (MEP) pathway, and/or that CIP has substantial activity unrelated to the apicoplast. Previous studies with *P. falciparum* have demonstrated the ability of fluoroquinolones to capture type II topoisomerase complexes with nuclear DNA, and for CIP in particular there is additional toxicity unrelated to nuclear or apicoplast topoisomerases (35).

Simply by changing the shape of the AUC from a concentration-intensive rapidly cleared high peak to a time-intensive constant infusion significantly increases efficacy of the antibacterials against malaria *in vitro* (Fig. 3). Such time dependence has implications for the clinical use and the success of these drugs. For maximal utility against *P. falciparum*, the delayed death phenomenon dictates that trough plasma concentrations should exceed the MIC for at least two life cycles (96 h). The success of this strategy is borne out by clinical trials of clindamycin monotherapy against blood-stage malaria, where 450 mg given three times a day for three days (a 4,050-mg total dose) yielded 50% efficacy (43), whereas 300 mg twice daily for five days (a 3,000-mg total dose) was 100% effective (44). Prolonged exposure improves the outcome, despite a lower total dose. Additional clinical trials have confirmed that CLI monotherapy has a mean efficacy of 98% when given at least twice daily for at least 5 days (7). The basis for this is evident in PK simulations, where currently recommended TID dosing provides trough concentrations of free drug that remain above the MIC for some 96% of the time

(Fig. 4A). In critically ill patients, CLI efficacy may be improved by modifying the dosing to q8h (Fig. 4B) to eliminate the overnight trough.

CHL has been tested as presumptive therapy against bacterial meningitis in conjunction with antimalarial treatment (36), but our findings suggest that its antimalarial contribution in this dosing regimen is negligible (Fig. 4F) and that adequate antimalarial concentrations would invoke dose-limiting toxicity. The likely basis for suboptimal clinical efficacy of CIP against malaria, especially as monotherapy (37), is based on inadequate pharmacokinetics, with the drug concentration never reaching the MIC (Fig. 4G). With a 4-h half-life and q12h dosing regimen, boosting CIP concentrations to achieve acceptable trough levels would require a 25-fold increase in dose size, virtually guaranteeing dose-related toxicities. Fluoroquinolones with greater intrinsic activity against malaria parasites (35) and a longer plasma half-life may provide a clinically useful alternative.

The case of TET is particularly interesting. Simulations reveal the impact of between-patient variability and of dosing schedule. The same dosing regimen may succeed or fail, depending on the half-life of drug within an individual (Fig. 4C and D). However, even with a relatively long 11-h plasma half-life, QID dosing of TET does not provide therapeutic concentrations until the second day, and they regularly fall below the MIC after overnight dosing breaks. The use of an evenly split q6h regimen results in more sustained therapeutic concentrations, and the addition of an initial loading dose provides reliable therapeutic levels from the outset of therapy. The importance of obtaining therapeutic concentrations with the first dose of an anti-infective, especially in critically ill patients, is well recognized (45, 46), and for this purpose a loading dose is now standard for intravenous quinine (9). Given the class-wide nature of PK drivers, it is reasonable to expect that doxycycline, the preferred class member for antimalarial use, is also time-driven. Use of a loading dose and regular dosing intervals would be expected to optimize its efficacy in both prophylaxis and treatment, a recommendation previously made on the basis of clinical study results (22).

Our findings provide insights into the action of antibacterials against *P. falciparum*. All drugs tested demonstrate the expected delayed death phenotype *in vitro*, but rescue by IPP is highly variable—robust for CLI but marginal for CIP—suggesting that nonapicoplast targets contribute to drug efficacy. Most interestingly, time is the PK driver of efficacy for all four drugs, regardless of their specific molecular target and sometimes in contrast to their PK/PD relationship against bacteria. It would be worthwhile testing these findings with other strains, including drug-resistant parasites. *In silico* simulations of human PK using antimalarial dosing regimens, in conjunction with our *in vitro* PK/PD findings, provide a starting point for assessing current dosing regimens. They identify a basis for CLI's success as an antimalarial and suggest changes to improve clinical efficacy of TET and perhaps doxycycline against malaria parasites. Although antibacterials in malaria treatment are used as part of a combination (9), their suboptimal dosing would result in intermittent monotherapy by the partner drug. The results of these dynamic *in vitro* PK/PD studies are contingent, and more detailed experiments that include Monte Carlo simulations would identify target durations for time over the MIC, which may not necessarily be 100% (47, 48).

## MATERIALS AND METHODS

**Parasite cultivation.** For all experiments, *P. falciparum* NF54 HOX (ATCC) was maintained (37°C and 5% CO<sub>2</sub> in air) asynchronously in phenol red-free RPMI with 4.4 μM hypoxanthine, 50 mM HEPES, 27 mM NaHCO<sub>3</sub>, in O<sup>+</sup> erythrocytes and 0.5% (wt/vol) Albumax II (Invitrogen) at 1.2 or 2.4% hematocrit and 0.25 to 6% parasitemia (20). Erythrocytes were obtained weekly from healthy donors under an Institutional Review Board-approved protocol. Parasitemia (infected/total erythrocytes) was determined by fluorescence microscopy of acridine orange-stained thin smears, examined until ≥50 infected cells or ≥2,000 total red cells were counted (49).

**Drugs.** Choice was based on obtaining a selection of therapeutic classes; on previous reports of use in human malaria, either as direct treatment or as adjunctive treatment in bacterial coinfection; and on commercial availability of radiolabeled tracer. Stocks were stored in aliquots at -20°C: 100 mM clindamycin hydrochloride (Sigma, PHR1159) and 15 mM tetracycline hydrochloride (Sigma, T7660) in water; 40 mM ciprofloxacin hydrochloride (Santa Cruz Biotechnology, SC29064) in 100 mM NaOH; and 600 mM chloramphenicol (Sigma, C0378), 640 μM artesunate (Sigma, D7439), and 500 μM artemisinin (Toronto Research Chemicals, A777500) in dimethyl sulfoxide. Tracers (Moravek, Inc.) were [<sup>3</sup>H]clindamycin

hydrochloride (1.0 Ci/mmol), [7-<sup>3</sup>H]tetracycline (11.6 Ci/mmol), [dichloroacetyl-1,2-<sup>14</sup>C]-D-threo-chloramphenicol (100 mCi/mmol), and [2-<sup>14</sup>C]ciprofloxacin (57.3 mCi/mmol).

**Antimalarial cytotoxicity assays.** In microtiter plate-based assays, parasites were exposed for 72 or 96 h, as indicated, to serial dilutions of drug (in quadruplicate), [<sup>3</sup>H]hypoxanthine was added for the final 24 h, and incorporation of radiolabel was evaluated (49–51). For 72-h assays, the starting conditions were 0.25% parasitemia, 1.2% hematocrit; for 96-h assays, they were 0.1% parasitemia, 1.2% hematocrit. For IPP rescue, at the start of the assay the medium was supplemented with 200 μM IPP (Tris-ammonium salt; Echelon Biosciences, I-0050). EC<sub>50</sub> values were determined by nonlinear curve fitting (Prism 6.0; GraphPad [see also the statistical analyses below]).

**Identifying kinetic driver.** Governing PK parameter (concentration or time of exposure) was determined as described previously (20, 49). Briefly, *P. falciparum* was seeded into three glass cartridges and maintained (via exchange through dialysis tubing) with continuously flowing medium. One cartridge was a no-drug control, and the other two were treated with the same total dose and AUC of drug, as either a high, rapidly cleared bolus (concentration-driven regimen) or a low constant infusion (time-driven regimen) (Fig. 1A). User-programmed drug kinetics were obtained by a series of pumps and reservoirs (Fig. 1B). Design of the apparatus and construction of the custom glass cartridge system have been described in detail (49).

For a given experiment, the infusion concentration was programmed at EC<sub>40</sub> from microtiter plate assays; values for 72- or 96-h cartridge studies were derived from plate assays of corresponding durations. The bolus regimen was calculated to provide the same total dose and AUC, via a single peak with a 4-h half-life that results in 98% drug elimination by 24 h. Programmed pharmacokinetics were confirmed using radioactive drug tracer in samples obtained over time from the cell compartment. Experiments were conducted for 72 h (0.25% starting parasitemia in 1.2% hematocrit) or 96 h (0.1% starting parasitemia in 1.2% hematocrit). At the end of a study, the efficacy was assessed by comparison of cell count to that of the no-drug control. PK driver was assigned to the regimen with significantly greater efficacy.

**In silico pharmacokinetic simulations.** Free drug concentrations in plasma were simulated over a 96-h interval, when given at the dose and schedule recommended for, or tested in, malaria therapy (9, 36, 37), using PK parameters (C<sub>max</sub>, half-life, and protein binding) extracted from clinical studies (21). To derive the plasma concentrations, dose proportionality and near-instantaneous T<sub>max</sub> were assumed. The antimalarial MIC was assigned as five times the protein binding-adjusted EC<sub>50</sub> concentration from 96-h microtiter plate assay. Intervals between doses for TID and QID regimens were 5, 7, and 12 h and 4, 4, 4, and 12 h, respectively. Simulations were performed in Excel 2010 for PC (Microsoft).

**Statistical analyses.** Chauvenet's criterion was used to identify any statistical outliers among quadruplicates within a given experiment. Dose-response curves were then generated by fitting anti-malarial effect versus log drug concentration to a four-parameter sigmoidal function using a least-squares method based on the Marquardt algorithm (50–52), with linear regression analysis (Prism 6.0; GraphPad). The goodness of fit (R<sup>2</sup> value) was evaluated by examining residuals versus concentration. Relative to 1/y or 1/y<sup>2</sup> weighting, in 91% of cases best fit was obtained with no y weighting, and in 9% of cases weighting improved R<sup>2</sup> values by ≤0.01. Statistical significance of EC<sub>50</sub> values and of PD results was assessed by two-tailed, unpaired Student t test, on at least three independent experiments. All cited values are means ± the standard deviations of three or more determinations. The percent coefficient of variation (%CV) was calculated as follows: (standard deviation/mean) × 100.

## ACKNOWLEDGMENTS

We are grateful to Kirsten Meyer for stimulating discussions and Craig Hendrix for technical advice, Mary Barry for assistance with experimental logistics, and Sean Prigge and David Sullivan for their comments on the manuscript.

This study was supported by the National Institutes of Health (R01AI095453), the Johns Hopkins Malaria Research Institute Parasite Core Facilities, and the Bloomberg Philanthropies. The funders had no role in study design, data collection and interpretation, or the decision to submit the work for publication.

## REFERENCES

- World Health Organization. 2018. Factsheet on the world malaria report 2018. World Health Organization, Geneva, Switzerland. <https://www.who.int/malaria/publications/world-malaria-report-2018/report/en/>.
- Tilley L, Straimer J, Gnädig NF, Ralph SA, Fidock DA. 2016. Artemisinin action and resistance in *Plasmodium falciparum*. Trends Parasitol 32: 682–696. <https://doi.org/10.1016/j.pt.2016.05.010>.
- Van der Wielen Y. 1937. Casuïstische mededeelingen. Nederlands Tijdschrift Voor Geneeskunde 81:2905–2906.
- Diaz de León A. 1937. Primeros casos de paludismo tratados por un derivado de la sulfanilamida. Bol Oficina Sanit Panam 16:1039–1040.
- Coatney GR, Greenberg J. 1952. The use of antibiotics in the treatment of malaria. Ann N Y Acad Sci 56:1075–1081. <https://doi.org/10.1111/j.1749-6632.1952.tb22668.x>.
- Rieckmann KH. 1983. Falciparum malaria: the urgent need for safe and effective drugs. Annu Rev Med 34:321–335. <https://doi.org/10.1146/annurev.me.34.020183.001541>.
- Lell B, Kremsner PG. 2002. Clindamycin as an antimalarial drug: review of clinical trials. Antimicrob Agents Chemother 46:2315–2320. <https://doi.org/10.1128/aac.46.8.2315-2320.2002>.
- Gaillard T, Madamet M, Pradines B. 2015. Tetracyclines in malaria. Malar J 14:445. <https://doi.org/10.1186/s12936-015-0980-0>.
- Centers for Disease Control and Prevention. 2018. Malaria diagnosis and treatment in the United States. Centers for Disease Control and Prevention, Atlanta, GA. [https://www.cdc.gov/malaria/diagnosis\\_treatment/index.html](https://www.cdc.gov/malaria/diagnosis_treatment/index.html).
- Craig WA. 1998. Pharmacokinetic/pharmacodynamic parameters: rationale for antimicrobial dosing of mice and men. Clin Infect Dis 26:1–10. <https://doi.org/10.1086/516284>.
- Ambrose PG, Bhavnani SM, Rubino CM, Louie A, Gumbo T, Forrest A,

- Drusano GL. 2007. Pharmacokinetics-pharmacodynamics of antimicrobial therapy: it's not just for mice anymore. *Clin Infect Dis* 44:79–86. <https://doi.org/10.1086/510079>.
12. Drusano GL. 2004. Antimicrobial pharmacodynamics: critical interactions of “bug and drug.” *Nat Rev Microbiol* 2:289–300. <https://doi.org/10.1038/nrmicro862>.
  13. Wu B, Sy SKB, Derendorf H. 2014. Principles of applied pharmacokinetic-pharmacodynamic modeling, p 63–79. In Vinks AA, Derendorf H, Mouton JW (ed), *Fundamentals of antimicrobial pharmacokinetics and pharmacodynamics*. Springer, New York, NY.
  14. Andes DR, Lepak AJ. 2017. *In vivo* infection models in the preclinical pharmacokinetic/pharmacodynamic evaluation of antimicrobial agents. *Curr Opin Pharmacol* 36:94–99. <https://doi.org/10.1016/j.coph.2017.09.004>.
  15. Marshall EK, Jr. 1940. The present status and problems of bacterial chemotherapy. *Science* 91:345–350. <https://doi.org/10.1126/science.91.2363.345>.
  16. Eagle H, Fleischman R, Musselman AD. 1950. Effect of schedule of administration on the therapeutic efficacy of penicillin. *Am J Med* 9:280–299. [https://doi.org/10.1016/0002-9343\(50\)90425-6](https://doi.org/10.1016/0002-9343(50)90425-6).
  17. Prins JM, Buller HR, Kuijper EJ, Tange RA, Speelman P. 1993. Once versus three times daily gentamicin in patients with serious infections. *Lancet* 341:335–339. [https://doi.org/10.1016/0140-6736\(93\)90137-6](https://doi.org/10.1016/0140-6736(93)90137-6).
  18. Rybak MJ, Abate BJ, Kang SL, Ruffing MJ, Lerner SA, Drusano GL. 1999. Prospective evaluation of the effect of an aminoglycoside dosing regimen on rates of observed nephrotoxicity and ototoxicity. *Antimicrob Agents Chemother* 43:1549–1555. <https://doi.org/10.1128/AAC.43.7.1549>.
  19. Meyer KJ, Caton E, Shapiro TA. 2018. Model system identifies kinetic driver of Hsp90 inhibitor activity against African trypanosomes and *Plasmodium falciparum*. *Antimicrob Agents Chemother* 62. <https://doi.org/10.1128/AAC.00056-18>.
  20. Bakshi RP, Nenortas E, Tripathi AK, Sullivan DJ, Shapiro TA. 2013. Model system to define pharmacokinetic requirements for antimalarial drug efficacy. *Sci Transl Med* 5:205ra135. <https://doi.org/10.1126/scitranslmed.3006684>.
  21. Vinetz JM. 2018. Chemotherapy of malaria, p 969–986. In Brunton LL, Halal-Dandan R, Knollmann BC (ed), *Goodman & Gilman's the pharmacological basis of therapeutics*, 13th ed. McGraw-Hill, New York, NY.
  22. Newton PN, Chaulet J-F, Brockman A, Chierakul W, Dondorp A, Ruangveerayuth R, Looareesuwan S, Mounier C, White NJ. 2005. Pharmacokinetics of oral doxycycline during combination treatment of severe falciparum malaria. *Antimicrob Agents Chemother* 49:1622–1625. <https://doi.org/10.1128/AAC.49.4.1622-1625.2005>.
  23. Fichera ME, Roos DS. 1997. A plastid organelle as a drug target in apicomplexan parasites. *Nature* 390:407–409. <https://doi.org/10.1038/37132>.
  24. Chakraborty A. 2016. Understanding the biology of the *Plasmodium falciparum* apicoplast; an excellent target for antimalarial drug development. *Life Sci* 158:104–110. <https://doi.org/10.1016/j.lfs.2016.06.030>.
  25. Wilson RJM, Denny PW, Preiser PR, Rangachari K, Roberts K, Roy A, Whyte A, Strath M, Moore DJ, Moore PW, Williamson DH. 1996. Complete gene map of the plastid-like DNA of the malaria parasite *Plasmodium falciparum*. *J Mol Biol* 261:155–172. <https://doi.org/10.1006/jmbi.1996.0449>.
  26. Yeh E, DeRisi JL. 2011. Chemical rescue of malaria parasites lacking an apicoplast defines organelle function in blood-stage *Plasmodium falciparum*. *PLoS Biol* 9:e1001138. <https://doi.org/10.1371/journal.pbio.1001138>.
  27. Wu W, Herrera Z, Ebert D, Baska K, Cho SH, DeRisi JL, Yeh E. 2015. A chemical rescue screen identifies a *Plasmodium falciparum* apicoplast inhibitor targeting MEP isoprenoid precursor biosynthesis. *Antimicrob Agents Chemother* 59:356–364. <https://doi.org/10.1128/AAC.03342-14>.
  28. Goodman CD, Su V, McFadden GI. 2007. The effects of antibacterials on the malaria parasite *Plasmodium falciparum*. *Mol Biochem Parasitol* 152: 181–191. <https://doi.org/10.1016/j.molbiopara.2007.01.005>.
  29. Geary TG, Jensen JB. 1983. Effects of antibiotics on *Plasmodium falciparum* *in vitro*. *Am J Trop Med Hyg* 32:221–225. <https://doi.org/10.4269/ajtmh.1983.32.221>.
  30. Dahl EL, Rosenthal PJ. 2007. Multiple antibiotics exert delayed effects against the *Plasmodium falciparum* apicoplast. *Antimicrob Agents Chemother* 51:3485–3490. <https://doi.org/10.1128/AAC.00527-07>.
  31. Uddin T, McFadden GI, Goodman CD. 2017. Validation of putative apicoplast-targeting drugs using a chemical supplementation assay in cultured human malaria parasites. *Antimicrob Agents Chemother* 62: e01161-17. <https://doi.org/10.1128/AAC.01161-17>.
  32. McKee EE, Ferguson M, Bentley AT, Marks TA. 2006. Inhibition of mammalian mitochondrial protein synthesis by oxazolidinones. *Antimicrob Agents Chemother* 50:2042–2049. <https://doi.org/10.1128/AAC.01411-05>.
  33. Chatzispayrou IA, Held NM, Mouchiroud L, Auwerx J, Houtkooper RH. 2015. Tetracycline antibiotics impair mitochondrial function and its experimental use confounds research. *Cancer Res* 75:4446–4449. <https://doi.org/10.1158/0008-5472.CAN-15-1626>.
  34. Kalghatgi S, Spina CS, Costello JC, Liesa M, Morones-Ramirez JR, Slomovic S, Molina A, Shirihai OS, Collins JJ. 2013. Bactericidal antibiotics induce mitochondrial dysfunction and oxidative damage in mammalian cells. *Sci Transl Med* 5:192ra85. <https://doi.org/10.1126/scitranslmed.3006055>.
  35. Tang Girdwood SC, Nenortas E, Shapiro TA. 2015. Targeting the gyrase of *Plasmodium falciparum* with topoisomerase poisons. *Biochem Pharmacol* 95:227–237. <https://doi.org/10.1016/j.bcp.2015.03.018>.
  36. Kokwaro GO, Muchohi SN, Ogutu BR, Newton CR. 2006. Chloramphenicol pharmacokinetics in African children with severe malaria. *J Trop Pediatr* 52:239–243. <https://doi.org/10.1093/tropej/fmi082>.
  37. Watt G, Shanks GD, Edstein MD, Pavanand K, Webster HK, Wechgritaya S. 1991. Ciprofloxacin treatment of drug-resistant falciparum malaria. *J Infect Dis* 164:602–604. <https://doi.org/10.1093/infdis/164.3.602>.
  38. Agwuh KN, MacGowan A. 2006. Pharmacokinetics and pharmacodynamics of the tetracyclines including glycylicyclines. *J Antimicrob Chemother* 58:256–265. <https://doi.org/10.1093/jac/dkl224>.
  39. Saivin S, Houin G. 1988. Clinical pharmacokinetics of doxycycline and minocycline. *Clin Pharmacokinet* 15:355–366. <https://doi.org/10.2165/0003088-198815060-00001>.
  40. Meyer KJ, Meyers DJ, Shapiro TA. 2019. Optimal kinetic exposures for classic and candidate antitrypanosomals. *J Antimicrob Chemother*. <https://doi.org/10.1093/jac/dkz160>.
  41. Ferri KF, Kroemer G. 2001. Organelle-specific initiation of cell death pathways. *Nat Cell Biol* 3:E255–E263. <https://doi.org/10.1038/ncb1101-e255>.
  42. Feagin JE. 1992. The 6-kb element of *Plasmodium falciparum* encodes mitochondrial cytochrome genes. *Mol Biochem Parasitol* 52:145–148. [https://doi.org/10.1016/0166-6851\(92\)90046-m](https://doi.org/10.1016/0166-6851(92)90046-m).
  43. Hall AP, Doberstyn EB, Nanokorn A, Sonkom P. 1975. Falciparum malaria semi-resistant to clindamycin. *Br Med J* 2:12–14. <https://doi.org/10.1136/bmj.2.5961.12>.
  44. Salazar NP, Saniel MC, Estoque MH, Talao FA, Bustos DG, Palogan LP, Gabriel AI. 1990. Oral clindamycin in the treatment of acute uncomplicated falciparum malaria. *Southeast Asian J Trop Med Public Health* 21:397–403.
  45. McKenzie C. 2011. Antibiotic dosing in critical illness. *J Antimicrob Chemother* 66(Suppl 2):ii25–31. <https://doi.org/10.1093/jac/dkq516>.
  46. Martinez MN, Papich MG, Drusano GL. 2012. Dosing regimen matters: the importance of early intervention and rapid attainment of the pharmacokinetic/pharmacodynamic target. *Antimicrob Agents Chemother* 56:2795–2805. <https://doi.org/10.1128/AAC.05360-11>.
  47. Louie A, Bied A, Fregeau C, Van Scoy B, Brown D, Liu W, Bush K, Queenan AM, Morrow B, Khashab M, Kahn JB, Nicholson S, Kulawy R, Drusano GL. 2010. Impact of different carbapenems and regimens of administration on resistance emergence for three isogenic *Pseudomonas aeruginosa* strains with differing mechanisms of resistance. *Antimicrob Agents Chemother* 54:2638–2645. <https://doi.org/10.1128/AAC.01721-09>.
  48. Louie A, Vanscoy B, Liu W, Kulawy R, Drusano GL. 2013. Hollow-fiber pharmacodynamic studies and mathematical modeling to predict the efficacy of amoxicillin for anthrax postexposure prophylaxis in pregnant women and children. *Antimicrob Agents Chemother* 57:5946–5960. <https://doi.org/10.1128/AAC.02616-12>.
  49. Caton E, Nenortas E, Bakshi RP, Shapiro TA. 2016. Hollow-fiber methodology for pharmacokinetic/pharmacodynamic studies of antimalarial compounds. *Curr Protoc Chem Biol* 8:29–58. <https://doi.org/10.1002/9780470559277.ch150194>.
  50. Desjardins RE, Canfield CJ, Haynes JD, Chulay JD. 1979. Quantitative assessment of antimalarial activity *in vitro* by a semiautomated microdilution technique. *Antimicrob Agents Chemother* 16:710–718. <https://doi.org/10.1128/aac.16.6.710>.
  51. Posner GH, Gonzalez L, Cumming JN, Klindedst D, Shapiro TA. 1997. Synthesis and antimalarial activity of heteroatom-containing bicyclic endoperoxides. *Tetrahedron* 53:37–50. [https://doi.org/10.1016/S0040-4020\(96\)00975-1](https://doi.org/10.1016/S0040-4020(96)00975-1).
  52. Bard Y. 1974. *Nonlinear parameter estimation*. Academic Press, New York, NY.
  53. Burgess DS, Frei CR, Lewis JS, Fiebelkorn KR, Jorgensen JH. 2007. The contribution of pharmacokinetic-pharmacodynamic modelling with Monte Carlo simulation to the development of susceptibility breakpoints for *Neisseria meningitidis*. *Clin Microbiol Infect* 13:33–39. <https://doi.org/10.1111/j.1469-0691.2006.01617.x>.